Excitonic Insulator State in Ta_2NiSe_5 Probed by Photoemission Spectroscopy

Y. Wakisaka,[1] T. Sudayama,[1] K. Takubo,[1] T. Mizokawa,[1,2] M. Arita,[2] H. Namatame,[2] M. Taniguchi,[2,3] N. Katayama,[4,*] M. Nohara,[4,†] and H. Takagi[4]

[1]*Department of Physics and Department of Complex Science and Engineering, University of Tokyo, Kashiwa, Chiba 277-8561, Japan*
[2]*Hiroshima Synchrotron Radiation Center, Hiroshima University, Higashi-Hiroshima 739-0046, Japan*
[3]*Graduate School of Science, Hiroshima University, Higashi-Hiroshima 739-8526, Japan*
[4]*Department of Advanced Materials, University of Tokyo, Kashiwa, Chiba 277-8561, Japan*

(Received 10 February 2009; published 10 July 2009)

We report on a photoemission study of Ta_2NiSe_5 that has a quasi-one-dimensional structure and an insulating ground state. Ni $2p$ core-level spectra show that the Ni $3d$ subshell is partially occupied and the Ni $3d$ states are heavily hybridized with the Se $4p$ states. In angle-resolved photoemission spectra, the valence-band top is found to be extremely flat, indicating that the ground state can be viewed as an excitonic insulator state between the Ni $3d$–Se $4p$ hole and the Ta $5d$ electron. We argue that the high atomic polarizability of Se plays an important role to stabilize the excitonic state.

DOI: 10.1103/PhysRevLett.103.026402 PACS numbers: 71.35.Lk, 71.30.+h, 79.60.−i

The idea of an excitonic insulator was theoretically proposed to be realized in a semiconductor or in a semimetal having a very small band gap E_G [1,2]. A very low carrier concentration results in weakly screened Coulomb interaction between a hole and an electron leading to an electron-hole bound state or an exciton. If the exciton binding energy E_B exceeds the magnitude of E_G, then the semiconducting or semimetallic ground state becomes unstable against the coherent formation of excitons, and the new ground state is called an excitonic insulator. A transition from a semiconductor to an excitonic insulator is characterized by a Bose-Einstein condensation of excitons while a semimetal undergoes a BCS-like transition to an excitonic insulator [3]. Because of excitonic coupling between the valence-band top and conduction-band bottom, which are separated by a wave vector of $\boldsymbol{w}$ in reciprocal space, an excitonic insulator is often accompanied by a new long range order with periodicity of $2\pi/|\boldsymbol{w}|$.

However, actual compounds studied from the viewpoint of excitonic insulator states are numbered. One example is $1T$-$TiSe_2$ which undergoes a $2 \times 2 \times 2$ charge-density-wave transition at around 200 K [4] and is attracting further interests due to the recent discovery of superconductivity induced by intercalation of copper [5]. Thus, many experimental works including angle-resolved photoemission spectroscopy (ARPES) have been performed on $1T$-$TiSe_2$, and the ARPES data have been analyzed in relevance to the excitonic insulator transition and its relation to the superconductivity [6–9]. Another candidate is Tm(Se,Te) that is also reported to undergo a transition to an excitonic insulator state by applying pressure [10].

Very recently, inspired by the discovery of superconductivity in Fe arsenides [11], Sawatzky *et al.* have proposed a new pairing mechanism due to the screening effect of anions with high atomic polarizability [12]. Since selenium or arsenic atoms have relatively large atomic polarizability, local Coulomb interaction between electrons (or holes) tends to be well screened in selenides or arsenides compared to oxides. On the other hand, screening of electron-hole interaction is expected to be more insensitive to the change of anion polarization than that of electron-electron and hole-hole interaction since the electron-hole pair does not produce local net charges either positive or negative. This situation benefits the formation of excitonic insulator states, and such a chemical trend is consistent with the fact that the candidates for excitonic inslulators are mainly selenides. In this view, transition-metal chalcogenides seem to be more promising than oxides for realizing new excitonic insulator states.

In the present work, we introduce Ta_2NiSe_5 as a new candidate for this excitonic insulator phase. We analyze the electronic structure of Ta_2NiSe_5 by means of x-ray photoemission spectroscopy (XPS) and ARPES, and conclude that the ground state of Ta_2NiSe_5 is characterized by the excitonic coupling between the Ni $3d$–Se $4p$ hole and the Ta $5d$ electron at the Γ point.

Ta_2NiSe_5 has a layered structure stacked loosely by van der Waals interaction. In each layer, nickel single chains and tantalum double chains are running along the a axis and aligned alternately along the c axis forming a quasi-one-dimensional structure. Selenium atoms are coordinated around the nickel atoms tetrahedrally and/or around the tantalum atoms octahedrally (see Fig. 1).

Its resistivity shows a metal-like behavior above 550 K while it becomes semiconductor-like below 500 K with an anomaly at 328 K which is attributed to a structural (martensitic) phase transition [13]. Magnetic susceptibility exhibits diamagnetism with an anomaly at the same temperature found in the resistivity. Although it is well known that many tantalum chalcogenides undergo phase transitions accompanying charge-density-wave (CDW) orders [14], they are not found in this system. In spite of the

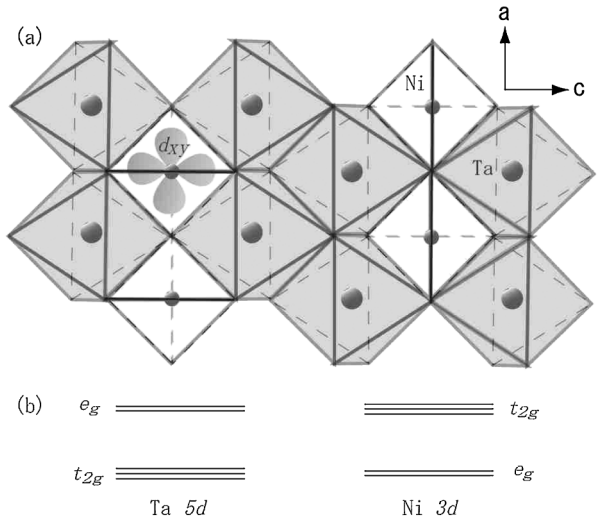

FIG. 1. (a) Crystalline structure of Ta_2NiSe_5 for one layer. The nickel and tantalum atoms are denoted as large and small spheres, respectively. Selenium atoms are supposed to be located at the vertices of the shaded octahedra. (b) Illustration of the energy level splitting for the tantalum and nickel sites whose symmetries are assumed to be octahedral (O_h) and tetrahedral (T_d), respectively.

usually expected formal valence of nickel (Ni^{2+}, $3d^8$) and tantalum (Ta^{4+}, $5d^1$), its semiconducting resistivity and diamagnetism suggest the absence of unpaired electrons, which forces us to formulate two different pictures for the electronic structure. The first scenario is to assume nickel to be $Ni^{0+}(3d^{10})$ that leaves tantalum to be $Ta^{5+}(5d^0)$. This view is corroborated by a tight-binding calculation [15] although the coexistence of low oxidized nickel and highly oxidized tantalum seems unlikely. The second one is the pairing of lone electrons in Ni^{2+} sites and in their two adjacent Ta^{4+} sites to form a Ta-Ni-Ta singlet [16].

Single crystals of Ta_2NiSe_5 were cleaved *in situ* for XPS and ARPES measurements. XPS was performed at room temperature using a JPS9200 analyzer equipped with a monochromatized Al $K\alpha$ line ($h\nu = 1486.6$ eV) as a light source with an energy resolution of ~0.6 eV. ARPES was performed at beam line 9 A, Hiroshima Synchrotron Radiation Center using a Scienta R4000 analyzer with circularly polarized light of two photon energies $h\nu =$ 10 eV and 23 eV. The data were collected at several temperatures (from 40 K to 300 K) with an angular resolution of ~0.3° and energy resolutions of 15 meV for $h\nu = 10$ eV and of 26 meV for $h\nu = 23$ eV.

Figure 2 displays the Ta $4f$ core-level spectra obtained at 300 K and 40 K. In conventional layered tantalum dichalcogenides, the appearance of commensurate or incommensurate CDW results in splitting or broadening of their Ta $4f$ core-level spectra [17]. These tendencies are not observed in our data even at 40 K, implying that no clear charge-density modulation exists down to at last 40 K in Ta_2NiSe_5 consistent with the absence of CDW transition. Interestingly, the Ta $4f$ core-level peaks show an asymmetric Doniach-Sunjic type line shape caused by metallic screening effect. In excitonic insulators, the band gap is created by the exciton formation due to the attractive Coulomb interaction between the valence-band holes and the conduction-band electrons. In the final state of the core-level photoemission process, the core hole attracts the electrons to the core-hole site and repels the holes from the core-hole site and would destroy the excitons. Therefore, metallic screening effect can be recovered around the core-hole site to provide the Doniach-Sunjic line shape.

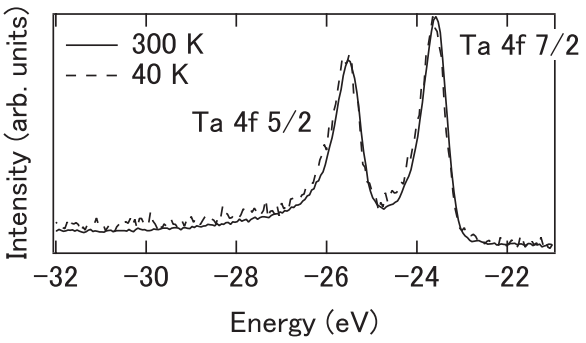

FIG. 2. Ta $4f$ core-level spectra of Ta_2NiSe_5 at 300 K (solid curve) and at 40 K (broken curve).

Figure 3 shows the Ni $2p_{3/2}$ core-level spectrum (solid curve) taken at 300 K and 40 K. Together with the main

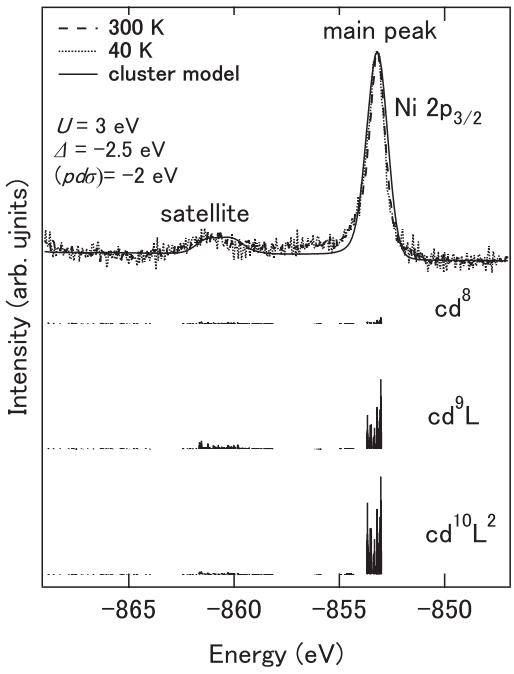

FIG. 3. Ni $2p_{3/2}$ core-level spectra of Ta_2NiSe_5 at 300 K (broken curve) and at 40 K (dotted curve). Experimental Ni $2p$ spectra along with the broadened calculated spectrum (solid curve) obtained from the $NiSe_4$ cluster calculation are shown in the upper panel. In the lower panel, the calculated line spectrum is decomposed into cd^8, cd^9L, and $cd^{10}L^2$ components.

sharp peak at −853 eV, the small satellite structure can be readily seen at around −861 eV. The satellite structures at 8 eV below the main peaks are observed in the Ni $2p$ core-level spectra and are not seen in the Ta $4f$ core-level spectra. Therefore, it is reasonable to assign the satellite to the charge-transfer satellite. The existence of a transition-metal $2p$ charge-transfer satellite is an earmark for partially occupied $3d$ orbitals [18]. Indeed, the experimental data was successfully reproduced by a $NiSe_4$ cluster-model calculation assuming the Ni formal valence to be +2. The calculated result with $U = 3$ eV, $\Delta = -2.5$ eV, and $(pd\sigma) = -2$ eV is indicated by the solid curve in Fig. 3. Here U, Δ, $(pd\sigma)$ are the multiple-averaged d-d Coulomb interaction energy, the Se $4p$-to-Ni $3d$ charge-transfer energy, and the transfer integral written in the Slater-Koster manner [19–21].

In the present cluster model, the Coulomb interaction between the Ni $3d$ electrons are given by the Slater integrals $F^0(3d, 3d)$, $F^2(3d, 3d)$, and $F^4(3d, 3d)$. The average Ni $3d$–Ni $3d$ Coulomb interaction U is expressed by $F^0(3d, 3d)$ and is an adjustable parameter. $F^2(3d, 3d)$ and $F^4(3d, 3d)$ are fixed to 80% of the atomic Hartree-Fock values [22]. The Coulomb interaction between the Ni $2p$ core hole and the Ni $3d$ electron is expressed by the Slater integrals $F^0(2p, 3d)$, $F^2(2p, 3d)$, and $G^1(2p, 3d)$. The average Ni $2p$–Ni $3d$ Coulomb interaction Q is expressed by $F^0(2p, 3d)$ and is fixed to $U/0.8$ [19]. $F^2(2p, 3d)$ and $G^1(2p, 3d)$ are fixed to 80% of the atomic Hartree-Fock values [22].

The ground state with ${}^3T_2$ symmetry is given by a linear combination of d^8, d^9L, and $d^{10}L^2$ configurations where L denotes a hole in the Se $4p$ orbital. The final states are given by linear combinations of cd^8, cd^9L, and $cd^{10}L^2$ configurations where c denotes a Ni $2p$ core hole. The negative charge-transfer energy $\Delta = -2.5$ eV generally means that holes are already located at the itinerant Se $4p$ orbitals in the ground state. In fact, the number of Ni $3d$ electrons is calculated to be 9.1, suggesting a strong d^9L character of the ground state. Here, it should be noted that the d^9L state has the ${}^3T_1$ symmetry in which the Ni $3d$ hole and the Se $4p$ hole form a spin triplet, and that the Ni formal valence is +2.

Although, in the usual sense, the itinerant Se $4p$ holes of the d^9L ground state contribute to metallic behaviors, the insulating state of Ta_2NiSe_5 could be explained by considering the formation of the Ta^{4+}-Ni^{2+}-Ta^{4+} singlet, the idea introduced previously. In this scenario, the two holes in the Ni $3d$–Se $4p$ hybridized band and the two electrons in the Ta $5d$ band form the singlet state. The Ta^{4+}-Ni^{2+}-Ta^{4+} singlet formation is consistent with the excitonic insulator mechanism, that is the creation of singlet excitons between holes at the Ni $3d$–Se $4p$ valence band and electrons at the Ta $5d$ conduction band. In other words, an excitonic insulator phase is realized in Ta_2NiSe_5 preventing its metallic conductivity. The tendency of an excitonic insulator is also manifested in the following ARPES results.

Figures 4(a)–4(d) show the ARPES results measured at 40 K with probing photon energies of 10 eV and 23 eV along X-Γ-X direction (parallel to the chain direction). Since Ta_2NiSe_5 has two Ni chains in the unit cell (see Fig. 1), the coupling between the two Ni chains is expected to give the band splitting as predicted by the band structure calculation [15]. The two bands split by the chain-chain coupling are clearly seen near the Γ point: the inner band (with bonding character) and the outer band (with antibonding character) are each well observed at $h\nu = 10$ eV and 23 eV but suppressed at the other due to the transition-matrix-element effect. Triangle and circle markers added in the second energy derivative plot mark the approximate peak positions of the two bands estimated by second derivative peak positions of its momentum distribution curve (MDC) and energy distribution curve (EDC) curves, respectively. Interestingly, the band dispersion of the outer band is very flat near the Γ point, and the flat band dispersion cannot be obtained by the band structure calculation [15]. In addition, in the ARPES data taken at 300 K [Figs. 4(e) and 4(f)], the flat and sharp outer band observed at 40 K is broadened and shifted towards the Fermi level

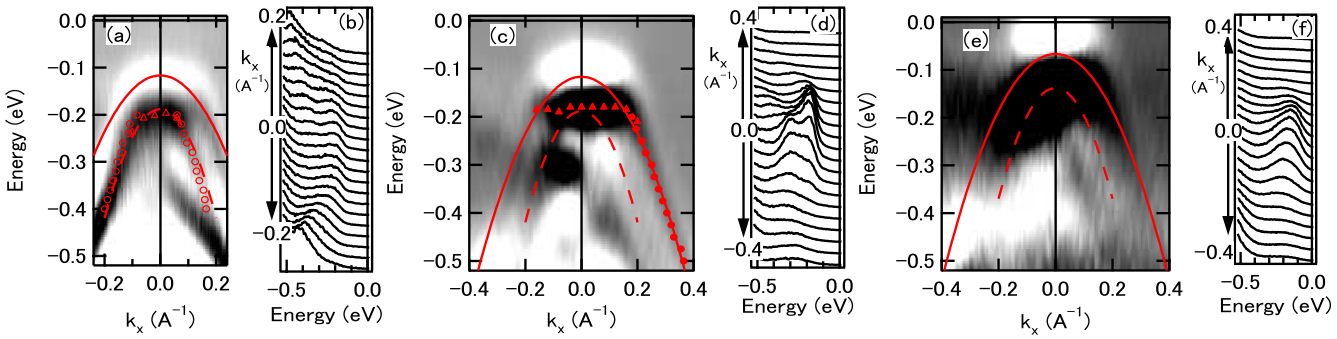

FIG. 4 (color online). ARPES results for Ta_2NiSe_5. (a) and (b) are the second energy derivative plot and the EDC plot, respectively, obtained at 40 K and $h\nu = 10$ eV, while (c) and (d) are the counterparts obtained at 40 K and $h\nu = 23$ eV. Open triangles and circles indicate the peak positions of the bands estimated by the second derivative of EDC and MDC data of $h\nu = 10$ eV, respectively, while the filled counterparts correspond to $h\nu = 23$ eV. Broken and solid curves are quadratic fits to the peak positions (see the text). (e) and (f) are the second energy derivative plot and the EDC plot, respectively, obtained at 300 K and $h\nu = 23$ eV.

indicating that 300 K is very close to the onset temperature of the excitonic insulator phase. In order to emphasize the flatness of the outer band at 40 K, we fitted the band dispersions obtained experimentally from the MDC curves (triangle markers) to quadratic functions $E_0 + \hbar^2 k^2/2m^*$ with two fitting parameters E_0 and m^*. As shown in the second energy derivative plots of Fig. 4, while the broken curve well reproduces the experimentally obtained inner band, the solid curve substantially deviates from the outer band near the Γ point.

This band flatness at 40 K is a characteristic of an excitonic insulator ground state and reported in a number of ARPES experiments of $Cu_xTi_{1-x}Se_2$ [6–9]. Here, it should be noted that the excitonic insulator state in Ta_2NiSe_5 is characterized by the absence of long range orders. Ta_2NiSe_5 is calculated to have a direct band gap at the Γ point [15] in contrast to $1T$-$TiSe_2$ whose valence-band top and conduction-band bottom are located at different points in the Brillouin zone [23], thus having no long range orders. If holes at the valence-band top, namely, the outer band seen in Fig. 4, can couple to electrons at the conduction-band bottom by the electron-hole Coulomb interaction and can form an excitonic insulator state, then the band dispersion of the valence-band top is expected to be flattened. As for Ta_2NiSe_5, the valence-band top is composed of Ni $3d$ t_{2g} and Se $4p$ orbitals while the conduction-band bottom is mainly constructed from the Ta $5d$ t_{2g} orbitals due to their different local symmetries [Fig. 1(b)]. In addition to the ARPES result, the relatively short distances between the Ni and Ta ions [13] is consistent with the exciton formation between the Ni $3d$–Se $4p$ hole and the Ta $5d$ electron.

In summary, the present XPS experiment and the cluster-model calculation for Ta_2NiSe_5 reveal that the unusual valence state is derived from the smallness of charge-transfer energy of the Ni site. Although the formal valence of the Ni site can be viewed as $+2$, the actual electronic configuration of the Ni site has the d^9L character, where L denotes a Se $4p$ hole. The flatness of the valence-band top revealed by the ARPES experiment strongly indicates that the excitonic insulator ground state is realized in Ta_2NiSe_5. The screening effect due to selenium with high atomic polarizability is probably important for the exciton formation between the Ni $3d$–Se $4p$ hole and the Ta $5d$ electron. The high polarizability of anions and the small charge-transfer energy of transition-metal ions are common between the present Ta_2NiSe_5 and the Fe-based superconductors such as $LaO_{1-x}F_xFeAs$. In addition, the excitonic effect has been proposed to be important to explain the spin density wave transition with orthorhombic structural distortion in LaOFeAs [24,25]. In the future, the electronic structure of various transition-metal selenides and arsenides should be studied systematically in the viewpoint of an excitonic insulator and its relation to superconductivity.

This work was supported by a global COE program "the Physical Sciences Frontier," from the Ministry of Education, Culture, Sports, Science, and Technology of Japan. The synchrotron radiation experiments have been done with the approval of Hiroshima Synchrotron Radiation Center (Proposals No. 06-A-49 and No. 08-A-2).

*Present address: Institute for Solid State Physics, University of Tokyo, Kashiwa, Chiba 277-8581, Japan
†Present address: Department of Physics, Okayama University, Tsushima-naka, Okayama 700-8530, Japan

[1] D. Jérome, T. M. Rice, and W. Kohn, Phys. Rev. **158**, 462 (1967).
[2] B. I. Halperin and T. M. Rice, Rev. Mod. Phys. **40**, 755 (1968).
[3] F. X. Bronold and H. Fehske, Phys. Rev. B **74**, 165107 (2006).
[4] F. J. DiSalvo, D. E. Moncton, and J. V. Waszczak, Phys. Rev. B **14**, 4321 (1976).
[5] E. Morosan *et al.*, Nature Phys. **2**, 544 (2006).
[6] Th. Pillo *et al.*, Phys. Rev. B **61**, 16 213 (2000).
[7] D. Qian *et al.*, Phys. Rev. Lett. **98**, 117007 (2007).
[8] J. F. Zhao *et al.*, Phys. Rev. Lett. **99**, 146401 (2007).
[9] H. Cercellier *et al.*, Phys. Rev. Lett. **99**, 146403 (2007).
[10] B. Bucher, P. Steiner, and P. Wachter, Phys. Rev. Lett. **67**, 2717 (1991).
[11] Y. Kamihara, T. Watanabe, M. Hirano, and H. Hosono, J. Am. Chem. Soc. **130**, 3296 (2008).
[12] G. A. Sawatzky, I. S. Elfimov, J. van den Brink, and J. Zaanen, arXiv:0808.1390.
[13] F. J. DiSalvo *et al.*, J. Less-Common Met. **116**, 51 (1986).
[14] J. A. Wilson, F. J. DiSalvo, and S. Mahasan, Adv. Phys. **24**, 117 (1975).
[15] E. Canadell and M.-H. Whangbo, Inorg. Chem. **26**, 3974 (1987).
[16] S. A. Sunshine and J. A. Ibers, Inorg. Chem. **24**, 3611 (1985).
[17] G. K. Wertheim, F. J. DiSalvo, and S. Chiang, Phys. Rev. B **13**, 5476 (1976).
[18] J. Ghijsen *et al.*, Phys. Rev. B **38**, 11322 (1988).
[19] K. Okada and A. Kotani, J. Phys. Soc. Jpn. **58**, 2578 (1989).
[20] T. Mizokawa *et al.*, Phys. Rev. B **52**, 13865 (1995).
[21] K. Takubo *et al.*, Phys. Rev. Lett. **99**, 037203 (2007).
[22] F. M. F. de Groot, J. C. Fuggle, B. T. Thole, and G. A. Sawatzky, Phys. Rev. B **42**, 5459 (1990).
[23] A. Zunger and A. J. Freeman, Phys. Rev. B **17**, 1839 (1978).
[24] V. Barzykin and L. P. Gorkov, arXiv:0806.1933.
[25] T. Mizokawa, T. Sudayama, and Y. Wakisaka, J. Phys. Soc. Jpn. **77**, Suppl. C, 158 (2008).